Analysis of the wind influence on the aerodynamic drag in the case of a certain emplacement of the pantograph on the electric rail vehicles

Sorin ARSENE*[,1], Ioan SEBESAN[1]

*Corresponding author
*[,1]"POLITEHNICA" University of Bucharest, Department of Railway Rolling Stock
Splaiul Independenţei 313, 060042, Bucharest, Romania
sorinarsene@gmail.com*, ioan_sebesan@yahoo.com

DOI: 10.13111/2066-8201.2015.7.1.1

Abstract: *The wind gusts with high speed can negative affect the operation of the railway electric vehicles. These vehicles can achieve high performances, as long as the power supply is ensured, without discontinuities or interruptions in the process. This work aims at conducting an analysis regarding the wind influence with regard to the energy collector placed on the vehicle bodywork taking in account a certain positioning of the active pantograph. To this end, in a first step, the EP3 pantograph which was raised to its maximum working height was 3-D modeled. As regards the simulation, we consider the case in which the equipment is placed on the vehicle so that the angle formed by the articulation of the arms is pointing in the direction of the air flow. The simulation is carried out for different points of the angles ranging between [0^o, 180^o] at the relative velocity of the fluid of 0m / s, 10m / s, 20m / s and 30m / s.*

Key Words: *pantograph air resistance, the influence of wind, air flow simulation, railway electric vehicles*

1. INTRODUCTION

Electric railway vehicles can move between two points located on a section of a railroad when the energy required for this purpose is taken from an external source, in this case from the line of contact (catenary). The equipment, through which a vehicle is supplied with energy from the catenary is called "pantograph" and is located on its bodywork. The layout and use of the collector (pantograph) increase the drag and implicitly the energy required to move the electric vehicle, compared to a vehicle powered from an internal source of energy (diesel vehicle), as can be seen and in papers [1-4].

The generalized formula for determining the running resistance for the railway vehicles, also known as Davis's relationship [1-11], is:

$$R_t = a + b \cdot v + c \cdot v^2 \tag{1}$$

where: R_t – the total resistance to motion of a vehicle; a – mechanical resistances to rolling caused by axle loads; $b \cdot v$ – non aerodynamic drag; $c \cdot v^2$ – aerodynamic drag; v – the vehicle rate of travel:

$$c = \frac{C_x \cdot S \cdot \rho}{2} \tag{2}$$

where: $C_x = 2 \cdot F_x / S \cdot \rho \cdot \bar{v}^{-2}$ – aerodynamic coefficient of air gliding, also known under the name of air penetration coefficient (dimensionless); S – the frontal area of the vehicle in the cross-sectional area (m^2); ρ – the air density in the moving vehicle (kg/m^3); F_x – drag frontal force (N); $\bar{v}$ – the speed of the fluid (air) (m/s).

Under normal displacement conditions the electric rail vehicles must overcome, the aerodynamic resistance generated by both the travel speed and the wind gusts.

In Romania, according to the data measured by the National Institute of Meteorology and Hydrology (NMA), the highest wind speed values were reached in February 1954 in Bucharest and at Iasi in the winter of 1966, namely 126km / h and 200km / h, respectively.

2. WIND INFLUENCE ON THE AERODYNAMIC DRAG GENERATED BY THE PANTOGRAPH

Two distinct situations, regarding the use of the active pantograph placed on the bodywork for the necessary electricity capturing can be found during the movement of the electric railway vehicles.

These two situations are determined by the position of the pantograph arms joint, as follows: when the pantograph arms joint determines an angle pointing to the air flow direction (fig. 1 a); when the joint between the lower and upper arm of the pantograph has the angle vertex oriented in the opposite direction of the air flow, (Fig. 1 b)

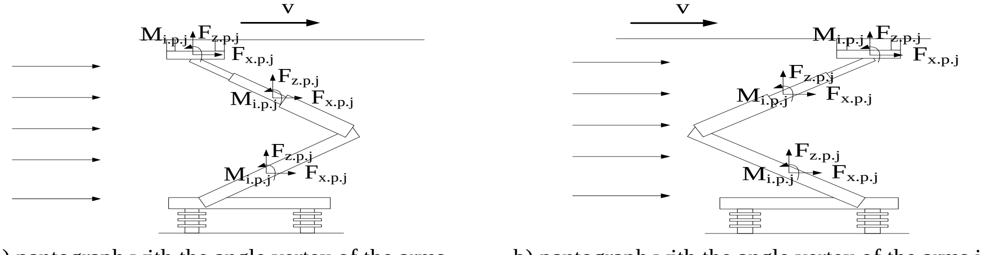

a) pantograph with the angle vertex of the arms joint pointing to the air flow direction

b) pantograph with the angle vertex of the arms joint pointing to the direction of the vehicle displacement

Fig. 1 – Method of the active pantograph arrangement

To determine the aerodynamic drag generated by the current collector article [18] presents a method based on the study of the equilibrium of forces and moments acting on the components of the pantograph.

According to this method the aerodynamic forces acting on the pantograph components are evaluated based on the corresponding aerodynamics coefficients as follows:

$$F_{xpj} = \frac{\rho \cdot \left(C_x \cdot S_p\right)_j \cdot v_{rel.p}^2}{2} \tag{3}$$

$$F_{zpj} = \frac{\rho \cdot \left(C_z \cdot S_p\right)_j \cdot v_{rel.p}^2}{2} \tag{4}$$

$$M_{ipj} = \frac{\rho \cdot \left(C_{mi} \cdot S_p \cdot l_p\right)_j \cdot v_{rel.p}^2}{2} \tag{5}$$

where: i – index of the Cartesian coordinate system axes; j – index of the pantograph components; F_{xpj}, F_{zpj} – aerodynamic forces on the longitudinal and vertical direction corresponding to each element of the pantograph; M_{ipj} – Moments determined on the pantograph components for each axis of the Cartesian system. $v_{rel.p}$ – relative incidence speed of the fluid flow through the pantograph elements; $\left(C_x \cdot S_p\right)_j$, $\left(C_z \cdot S_p\right)_j$ and $\left(C_M \cdot S_p \cdot l_p\right)_j$ – pressure coefficients of the aerodynamic frontal resistance, pressure coefficients of the aerodynamic frontal and vertical resistance, respectively and couples resulted for each j element in which the pantograph was divided.

The determination of the relative rate (relation 6), depending on the direction and angle in which blows the wind with respect to the longitudinal axis of the vehicle is shown in fig.2.

a) tail wind b) head wind

Fig. 2 – The influence of the wind depending on the angle and its direction

$$\mathrm{v_{rel}} = \mathrm{v} \pm \mathrm{v_v} \cdot \cos(\alpha) \tag{6}$$

where v – the speed of the vehicle; $\mathrm{v_v}$ – wind speed; α – the angle between the vehicle direction of movement and the wind speed.

In these conditions the coefficients of the aerodynamic force (relation 7) and moments (relation 8), respectively, generated by the air through the pantograph elements can be written as:

$$\mathrm{C_{ij}} = \frac{2 \cdot \mathrm{F_{ipj}}}{\mathrm{S_{pj}} \cdot \rho \cdot \mathrm{v_{rel}}^2} = \frac{2 \cdot \mathrm{F_{ipj}}}{\mathrm{S_{pj}} \cdot \rho \cdot \left(\mathrm{v} + \mathrm{v_v} \cdot \cos(\alpha)\right)^2} \tag{7}$$

$$\mathrm{C_{mij}} = \frac{2 \cdot \mathrm{M_{ipj}}}{\mathrm{S_{pj}} \cdot \mathrm{l_{ij}} \cdot \rho \cdot \mathrm{v_{rel}}^2} = \frac{2 \cdot \mathrm{M_{ipj}}}{\mathrm{S_{pj}} \cdot \mathrm{l_{ij}} \cdot \rho \cdot \left(\mathrm{v} + \mathrm{v_v} \cdot \cos(\alpha)\right)^2} \tag{8}$$

When the wind speed is geared towards the train movement (tail wind), the air resistance decreases or has a negative value.

Negative values occur only when the component of the equivalent speed determined by the wind is greater than the speed of the vehicle and has the same direction, as described in paper [19].

3. SIMULATION OF THE AIR FLOW THROUGH THE PANTOGRAPH ELEMENTS

For this simulation, we considered the design of the EP3 pantograph, which is used by most of the LE 060 EA 5100kW electric locomotives, operated by the railway companies from Romania.

I started by the geometric modeling of the equipment components at scale 1: 1, using Autodesk Inventor.

With these components, I realized assembly of the pantograph so that its patina is located at the maximum allowable height of 2.5m for the current capture, according to technical specifications.

In order to simulate the air flow through the components of the pantograph I used the SolidWorks Flow Simulation software.

In this paper, I considered for analysis only the first case of the active pantograph emplacement (fig. 1), where we took into account the relative velocity of the air when the vehicle is moving at a constant speed of 144km/h = 40m/s.

In terms of wind speed we successively considered the values of 0m/s and 10m/s, 20m/s, respectively 30m/s.

For the angle between the wind direction and the direction of movement of the vehicle, we successively considered the cases: 0^o, 30^o, 45^o, 60^o, 90^o, 120^o, 150^o and 180^o. 25 distinct cases to be analyzed resulted under the above-mentioned conditions.

These cases are given by the 8 different values of the wind angle, and for each case we considered three values of velocity and also the case when the vehicle is traveling in an area without wind gusts.

The delimitation of the volume of the air flow is carried out as follows: - for the vertical plan we considered the appropriate plan of the vehicle roof and another plan located at 6 m away from it; - for the cross section, we considered two plans located symmetrically at 5 m from the longitudinal plan of the vehicle; - for the longitudinal section, we considered two plans located at 5 and 10 m away from the transverse plan of the pantograph frame;

The first plan of the longitudinal section (at 5m) corresponds to the front of the locomotive in the air flow direction and the second plan of the same section (at 10m) corresponds to the back of the vehicle.

As input parameters regarding the atmospheric conditions we considered a pressure of 101325 Pa and a temperature of 293.2 K.

The distributions of the pressure exerted on the pantograph and the contour line for the dynamic pressure, which are resulted from the simulation of the 25 analyzed cases are presented in Figs. 3 and 4, respectively.

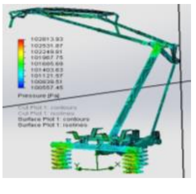

$\alpha=0^o - v_v=0$m/s

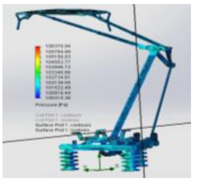

$\alpha=0^o - v_v=10$m/s

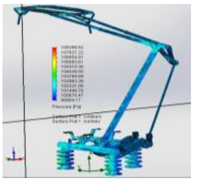

$\alpha=0^o - v_v=20$m/s

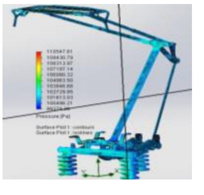

$\alpha=0^o - v_v=30$m/s

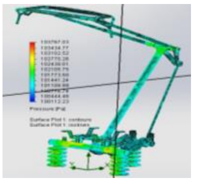

$\alpha=30^o - v_v=10$m/s

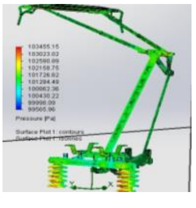

$\alpha=30^o - v_v=20$m/s

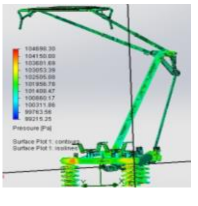

$\alpha=30^o - v_v=30$m/s

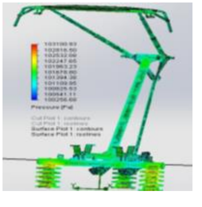

$\alpha=45^o - v_v=10$m/s

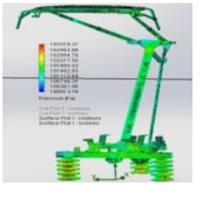

$\alpha=45^o - v_v=20$m/s

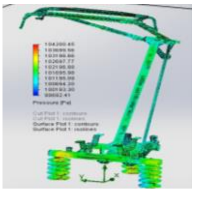

$\alpha=45^o - v_v=30$m/s

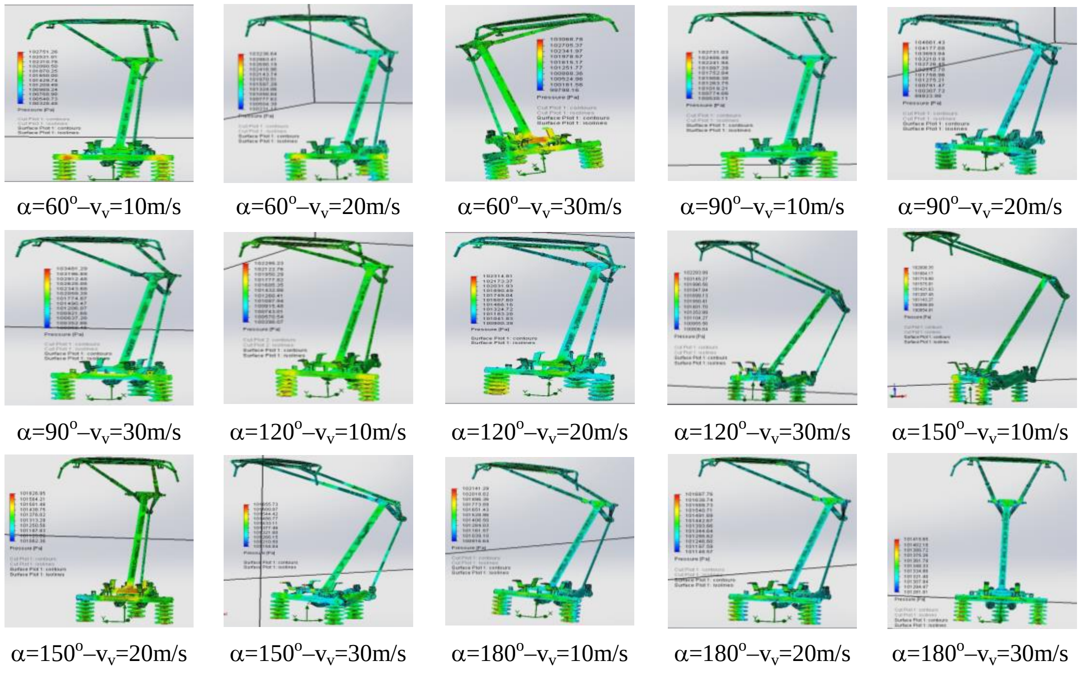

Fig. 3 – Pressure distribution on the surface of the pantograph

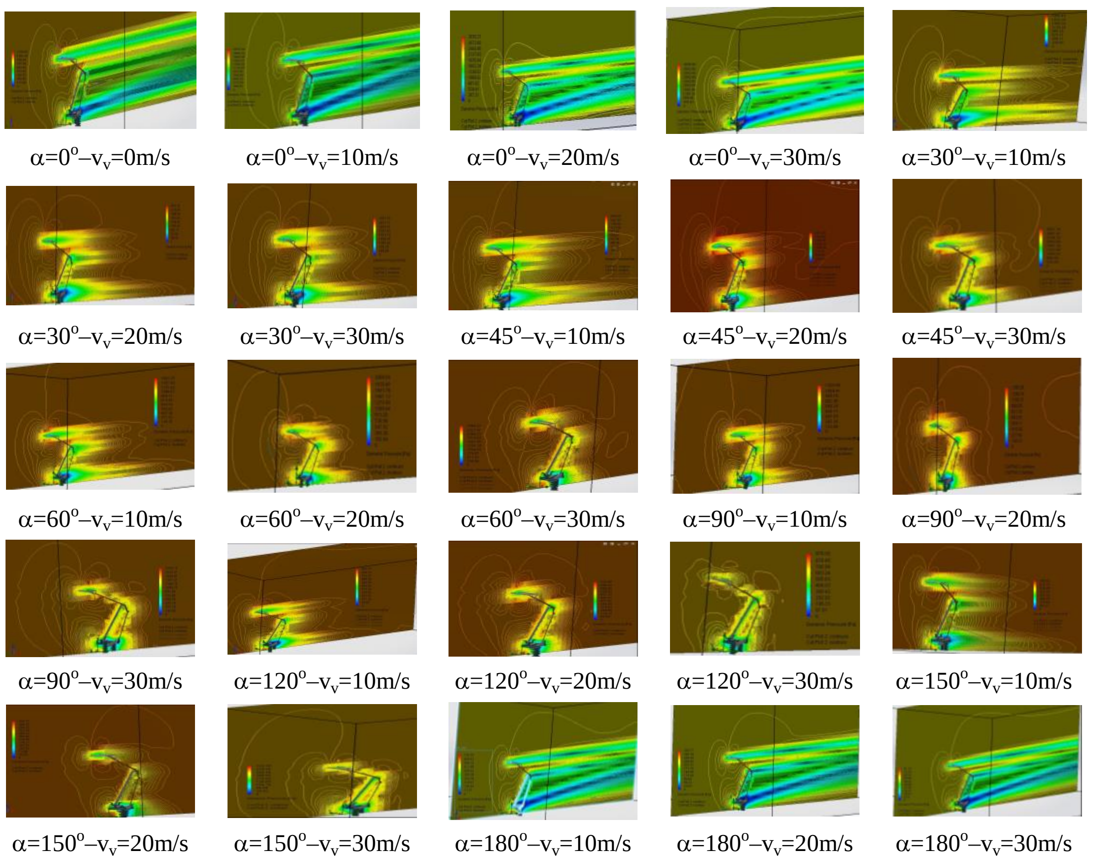

Fig. 4 – Contour lines of the dynamic pressure in the median longitudinal plane of the vehicle

The values of the total pressure and aerodynamic resistances obtained based on the air flow simulation of the analyzed cases are shown in Figures 5 and 6 taking into account the 8 values of the angles.

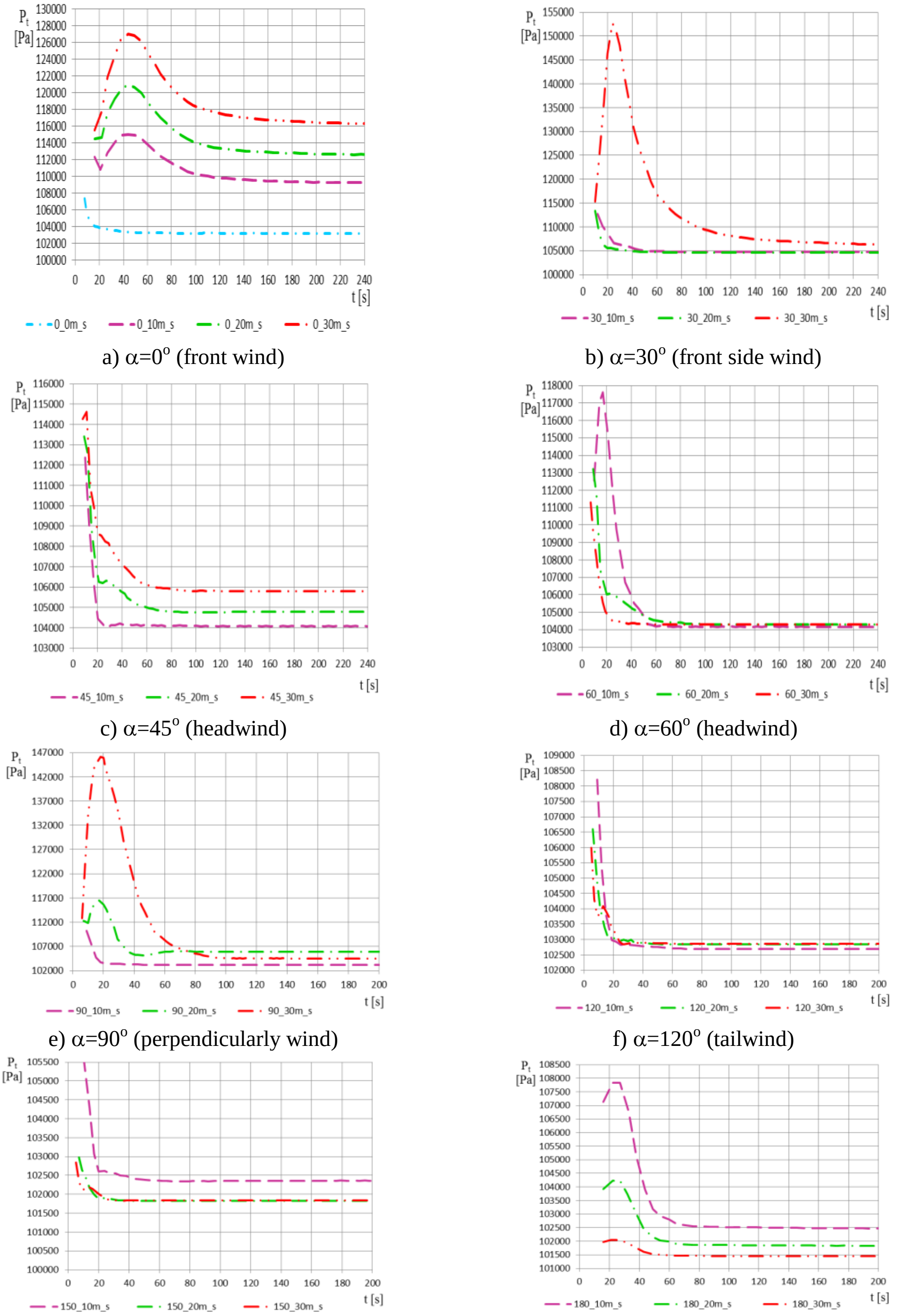

a) α=0^o (front wind)

b) α=30^o (front side wind)

c) α=45^o (headwind)

d) α=60^o (headwind)

e) α=90^o (perpendicularly wind)

f) α=120^o (tailwind)

g) α=150^o (tailwind)

h) α=180^o (tailwind)

Fig. 5 – Total pressure values obtained during the simulation

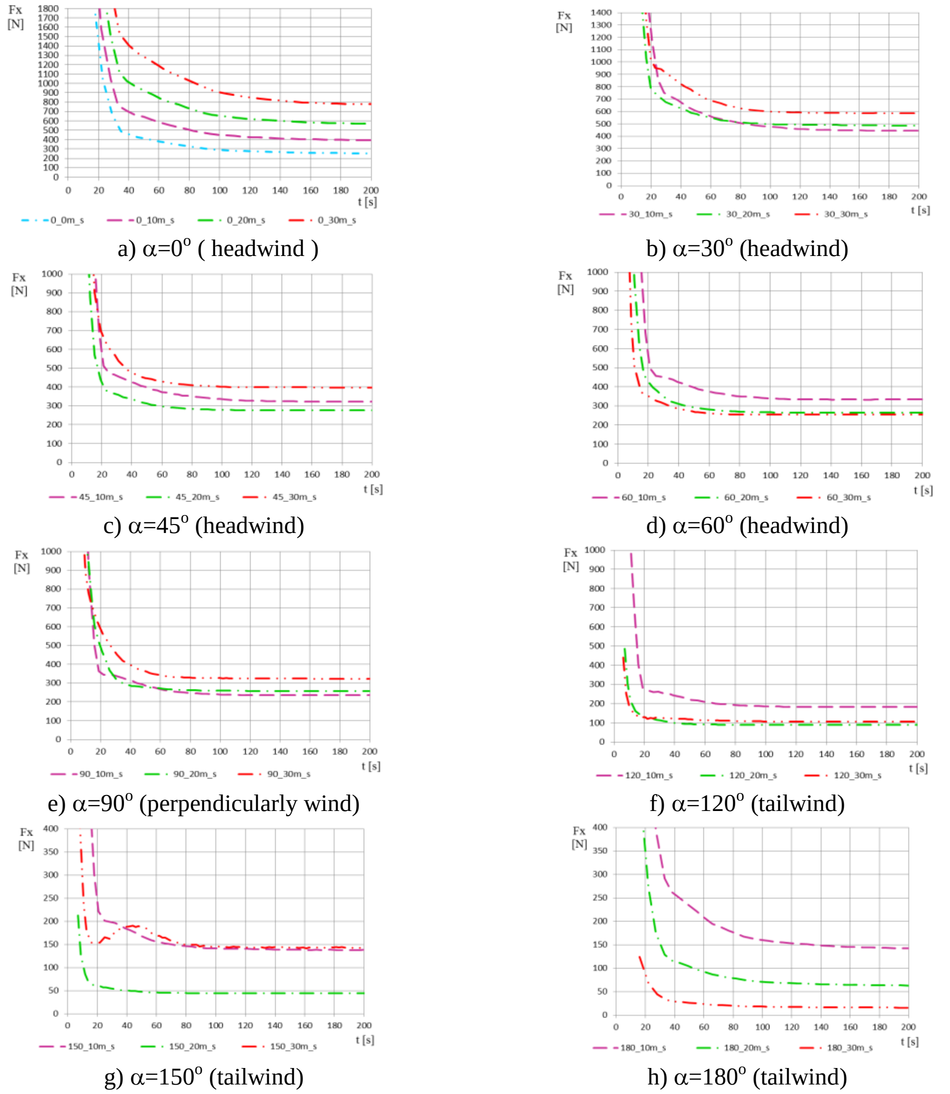

a) $\alpha=0^o$ (headwind) b) $\alpha=30^o$ (headwind)

c) $\alpha=45^o$ (headwind) d) $\alpha=60^o$ (headwind)

e) $\alpha=90^o$ (perpendicularly wind) f) $\alpha=120^o$ (tailwind)

g) $\alpha=150^o$ (tailwind) h) $\alpha=180^o$ (tailwind)

Fig. 6 – Variation of the aerodynamic resistance during simulation for the 8 values of the wind angles.

To assess the influence of the wind on the aerodynamic drag we performed a percentage analysis of the stabilized values obtained from simulations successively considering three types of values as a reference point, namely: - when the vehicle moves in atmospheric conditions without wind gusts (Fig. 7); - when the wind speed is 10 m / s (Fig. 8); - when the wind is frontal. (Fig. 9).

The stabilized values of the aerodynamic drag of the pantograph resulting from simulations are presented in Table 1.

Table 1 – Stabilized values of the F_x[N] pantograph aerodynamic drag

Angle / v_v[m/s]	0^o	30^o	45^o	60^o	90^o	120^o	150^o	180^o
0	278,7 [N]	-	-	-	-	-	-	-
10	398,1 [N]	444,1 [N]	320,9 [N]	339,5 [N]	236,1 [N]	186,5 [N]	137,1 [N]	140,9 [N]
20	572,6 [N]	491,9 [N]	277,2 [N]	274,7 [N]	262,6 [N]	88,9 [N]	44,3 [N]	62,6 [N]
30	780,4 [N]	592,7 [N]	409,8 [N]	252,4 [N]	298,3 [N]	158,8 [N]	51,1 [N]	15,6 [N]

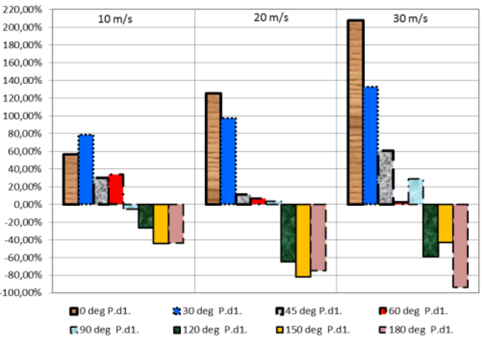

Fig. 7 –The percentage analysis of the aerodynamic drag generated by the pantograph, having as reference point, the resistance obtained when the vehicle is moving under atmospheric conditions without wind gusts

The largest percentage increase, to aerodynamic resistance values determined by the pantograph is given in the case of a front wind (Fig. 7). It reaches about tripling it for $\alpha=0^o$ – $v_v=30m/s$ (≈ 180%) towards the case when we do not have gust of wind. Considering the same benchmark, the lowest percentage of the resistance is obtained, as expected, for the case of a wind from behind, $\alpha=180^o$ – $v_v=30m/s$ (≈ –95%).

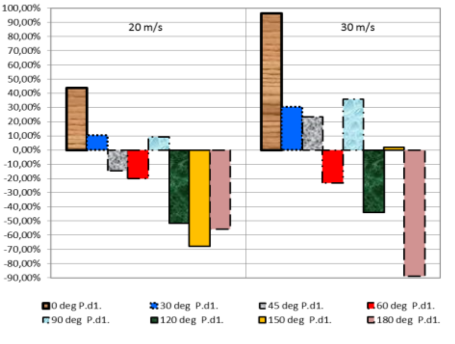

Fig. 8 – The percentage analysis of the aerodynamic drag generated by the pantograph, having as reference point the resistances obtained for a wind of 10m / s corresponding to each angle considered

Taking as a reference point for comparison, the lowest wind speeds for the angles examined (Fig. 8), it is found that the extreme values, for the percentage variation of the pantograph aerodynamic drag are obtained also for $\alpha=0^o$ – $v_v=30m/s$ (≈ 96%) - the maximum increase, respectively for $\alpha=180^o$ – $v_v=30m/s$ (≈ –89%) - maximum decrease.

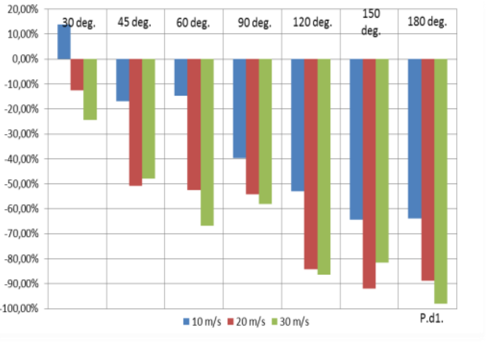

Fig. 9 –The percentage analysis of aerodynamic drag generated by the pantograph, having as reference point, the resistances obtained for a headwind

Considering the headwind case (Fig. 9) we can conclude that in this case the highest aerodynamic resistances of the pantograph and implicitly the highest consumption of energy required are obtained.

4. CONCLUSION

As expected, the wind has influence on the pressure values exerted on the pantograph and implicitly to its aerodynamic drag. From Fig. 6 a) and Fig. 6 h) it can be seen that: the extreme stabilized values resulting after simulation with respect to the aerodynamic drag of the pantograph are obtained in case of the high wind speeds.

When the wind is oriented against the direction of travel of the vehicle (headwind), we obtain the maximum value of resistance.

If it is oriented in the direction of travel (wind from behind) the minimum values of resistance. Thus leading to corresponding changes in the quantity of electricity consumed by the vehicle.

In the range of values considered for the angle (0^o – 180^o) formed between the wind direction and the longitudinal axis of the vehicle, considering the constant speed thereof, it follows that the stabilized values of the aerodynamic drag of the pantograph have decrease with the increase of the angle.

For the case when a constant angle and a wind speed variation are considered, the simulations resulted in a random distribution of the values of the pantograph aerodynamic drag. This distribution starts from a tendency to increase the resistance with the speed in the case of the headwind and gets up to a tendency to decrease the resistance with the speed when the wind blows from behind.

The first comparative percentage analysis regarding the aerodynamic drag of the pantograph (Fig. 7), when we take as a reference point the case of the vehicle movement in atmospheric conditions without wind gusts, reveals that in the interval ranging between 0° and 90° for the α angle largely positive values are obtained .

This means that wind gusts determine an increase of the aerodynamic resistance. For the rest of the interval ranging from 90 ° to 180 °, the values are mostly negative, which means a reduction in aerodynamic drag.

The same can also be observed for the second case of the comparative percentage analysis (Fig. 8), when the reference point is considered the resistance obtained for the lowest wind speed analyzed.

The last percentage analysis when the reference point is considered the case determined by a headwind (Fig. 9), reveals a downward trend to the aerodynamic resistance caused by the pantograph. Changing the wind speed and the angle in which it blows, determines the change of aerodynamic resistances of the pantograph and implicitly of the vehicle. In turn this causes further variations of the amount of energy required for moving the locomotive.

ACKNOWLEDGEMENT

This work is supported by the Sectorial Operational Programme Human Resources Development (SOP HRD), financed from the European Social Fund and the Romanian Government under the contract number POSDRU/159/1.5/S/137390.

This paper was presented at the International Conference of Aerospace Sciences “AEROSPATIAL 2014”, 18 - 19 September, Bucharest, Romania, to which additions were made.

REFERENCES

[1] S. Arsene, Teză de Doctorat - *Contribuţii privind îmbunătăţirea performanţelor de tracţiune ale vehiculelor electrice*, Universitatea Politehnica din Bucureşti, 2013.

[2] I. Sebeşan, S. Arsene, C. Stoica, Experimental study on determination of aerodynamic resistance to progress for electric locomotive LE 060 EA1 of 5100 kW, *Scientific Bulletin-University Politehnica of Bucharest*, Series D, vol. **75**, Issue. 4, p. 85-96, 2013.

[3] I. Sebesan, S, Arsene, C. Stoica, Experimental analysis for aerodynamic drag of the electric locomotives, *INCAS BULLETIN*, (online) ISSN 2247–4528, (print) ISSN 2066–8201, ISSN–L 2066–8201, vol. **5**, Issue 3, DOI: 10.13111/2066-8201.2012.5.3.11, pp.99-113, 2013.

[4] I. Sebesan, S. Arsene, Study on aerodynamic resistance to electric rail vehicles generated by the power supply, *INCAS BULLETIN*, (online) ISSN 2247–4528, (print) ISSN 2066–8201, ISSN–L 2066–8201, Volume **6**, Special Issue 1, DOI: 10.13111/2066-8201.2014.6.S1.17, pp. 151 – 158, 2014.

[5] R. S. Raghunathan, H.-D. Kim, T. Setoguch, Aerodynamics of high-speed railway train, *Progress in Aerospace Sciences*, vol. **38**, Issues 6–7, ISSN: 0376-0421, pp. 469–514, 2002.

[6] P. Lukaszewicz, Doctoral Thesis - *Energy Consumption and Running Time for Trains - Modelling of running resistance and driver behaviour based on full scale testing*, Department of Vehicle Engineering Royal Institute of Technology, KTH, Stockholm, 2001.

[7] A. Orellano, M. Schober, *Aerodynamic Performance of a Typical High-Speed Train*, in Proceedings of the 4th WSEAS International Conference on Fluid Mechanics and Aerodynamics, Elounda, Greece, August 21-23, pp. 18-25, 2006.

[8] P. Lukaszewicz, E. Andersson, *Green Train energy consumption Estimations on high-speed rail operations*, KTH Railway Group, Stockholm, ISBN 978-91-7415-257-9, Stockholm 2009.

[9] I. Sebeşan, S. Arsene, *Considerations on study the aerodynamic of pantographs railway vehicles*, in International Conference of Aerospace Sciences – "AEROSPATIAL 2012", Bucharest, 11-12 October, p.397-402, 2012.

[10] S. Arsene, *Analysis regarding the aerodynamic resistances on boxes electric locomotives*, in The International Conference on INnovation and Collaboration in Engineering Research – "INCER 2013", Bucharest, 20-21 June, pp. 157-160, 2013.

[11] I. Sebeşan, B. Tarus, Some aspects regarding the impact of aerodynamics on fuel consumption in railway applications, *U.P.B. Sci. Bull., Series D*, Vol. **73**, Iss. 4, p. 237-246, 2011.

[12] J. D. Anderson Jr., *Fundamentls of aerodynamics* – Second Edition, Ed. McGraw-Hill, 1991.

[13] I. Sebeşan, B. Ţarus, The impact of aerodynamics on fuel consumption in railway applications, *INCAS BULLETIN*, (online) ISSN 2247–4528, (print) ISSN 2066–8201, ISSN–L 2066–8201, Volume **4**, Issue 1, DOI: 10.13111/2066-8201.2012.4.1.10, pp. 93 – 102, 2012.

[14] L. Li, W. Dong, Y, Ji, Z. Zhang, A minimal-energy driving strategy for high-speed electric train, *J Control Theory*, vol. **10**, nr. 3, ISSN: 1672-6340 (Print) 1993-0623 (Online), DOI 10.1007/s11768-012-1129-0, pp. 280–286, Appl 2012.

[15] F. Cheli, F. Ripamonti, D. Rocchi, G. Tomasini, Aerodynamic behaviour investigation of the new EMUV250 train to cross wind, *Journal of Wind Engineering and Industrial Aerodynamics*, Volume **98**, Issues 4–5, ISSN: 0167-6105, pp. Pages 189–201, April–May 2010.

[16] F. Cheli, R. Corradi, D. Rocchi, G. Tomasini, E. Maestrini, Wind tunnel tests on train scale models to investigate the effect of infrastructure scenario, *Journal of Wind Engineering and Industrial Aerodynamics*, vol. **98**, nr. 6-7, ISSN: 0167-6105, doi:10.1016/j.jweia.2010.01.001, pp. 189–201, 2010.

[17] M. Schober, M. Weise, A. Orellano, P. Deeg, W. Wetzel, Wind tunnel investigation of an ICE3 endcar on three standard ground scenarios, *Journal of Wind Engineering and Industrial Aerodynamics*, Volume **98**, nr. Issues 6–7, ISSN: 0167-6105, DOI:10.1016/j.jweia.2009.12.004, Pages 345–352, June–July 2010.

[18] J. Pombo, J. Ambrósio, M. Pereira, F. Rauter, A. Collina, A. Facchinetti, Influence of the aerodynamic forces on the pantograph–catenary system for high-speed trains, *Vehicle System Dynamics*, Vol. *1* din Vol. **47**, No. 11, ISSN 0042-3114 (Print), 1744-5159 (Online), DOI:10.1080/00423110802613402, pp. 1327–1347, November 2009.

[19] R. Gregoire, A. Collina, F. Resta, D. Rocchi, *Some considerations on the aerodynamics of high speed pantograph: cfd and wind tunnel tests*, BBAA VI International Colloquium on: Bluff Bodies Aerodynamics & Applications, Milano, Italy, July, 20-24 2008.